

A Proton Conductor Showing an Indication of Single-ion Magnet Based on a Mononuclear Dy(III) Complex

Shui-Dong Zhu^a, Lu Dong^c, Jun-Jie Hu^a, He-Rui Wen^{*, a}, Ying-Bing Lu^c, Wei-Hua Deng^b,
Cai-Ming Liu^{*, d}, Shui-Jun Liu^a, Gang Xu^b and Zhi-Hua Fu^{*, b}

^a*School of Chemistry and Chemical Engineering, Jiangxi University of Science and Technology, Ganzhou 341000, Jiangxi Province, P.R. China.*

^b*State Key Laboratory of Structural Chemistry, Fujian Institute of Research on the Structure of Matter, Chinese Academy of Sciences, Fuzhou, Fujian 350002, P. R. China.*

^c*Jiangxi Key Laboratory of Function of Materials Chemistry, College of Chemistry and Chemical Engineering, Gannan Normal University, Ganzhou, 341000, P. R. China.*

^d*Beijing National Laboratory for Molecular Sciences, Center for Molecular Science, Key Laboratory of Organic Solids, Institute of Chemistry, Chinese Academy of Sciences, Beijing 100190, P. R. China.*

E-mail: wenherui63@163.com, zhihuafu@fjirsm.ac.cn, cmliu@iccas.ac.cn

CONTENTS

Table S1. X-ray Diffraction Crystallographic Data for **1**.

Table S2. Selected Bond Lengths (\AA) and Bond Angles ($^{\circ}$) for **1**.

Table S3. Summary of SHAPE analysis for **1**.

Table S4. H-bonding length and angle table for **1**.

Figure S1. Sphenocorona coordination polyhedron around the Dy^{III} ion in **1**.

Figure S2. 3-D supramolecular network of **1** formed by H-bond along the *c*-axis.

Figure S3. TGA plot of **1**.

Figure S4. PXRD patterns of simulated one, as-synthesized sample, the sample after proton conduction of **1**.

Figure S5. Nyquist plot for **1** at 25 $^{\circ}\text{C}$ under 100% RH.

Figure S6. Nyquist plot for **1** at 35 $^{\circ}\text{C}$ under 100% RH.

Figure S7. The photograph of crystals of complex **1** after exposed to 25-35 $^{\circ}\text{C}$ and 60-100% RH conditions during the whole proton conductivity measurements.

Table S5. Proton conductivity of **1** at 25 $^{\circ}\text{C}$ under variable relative humidity (RH).

Table S6. Comparison of the proton conductivity of **1** with that of imidazole/imidazole derivates-based conducting materials.

Figure S8. AC susceptibility measurements at frequency with 977 Hz for **1** at $H_{dc} = 0$ Oe, $H_{ac} = 2.5$ Oe.

Table S7. Linear combination of two modified debye model fitting parameters from 2 to 7 K at $H_{dc} = 2000$ Oe.

Table S8. The comparisons of the proton conductivity and the U_{eff}/k values of **1** with the previously reported proton-conductive nanomagnet.

Figure S9. IR spectra for **1**

Table 1. X-ray Diffraction Crystallographic Data for **1**.

Complex 1			
Formula	C ₁₂ H ₁₆ DyN ₁₁ O ₁₁	□ (mm ⁻¹)	3.747
Fw	652.86	F (000)	1276
Temp (K)	296(2)	Reflns collected	12586
Crystal system	Monoclinic	Independent reflns	1756
Space group	C2/c	R _{int}	0.0170
a, Å	14.3641(2)	Theta range, □	2.01-25.00
b, Å	15.5489(2)	Params/restraints/data	1756 / 3 / 168
c, Å	9.79550(10)	R ₁ [I > 2σ(I)]	0.0206
□, (deg)	111.0960(10)	wR ₂ (all data)	0.0498
V, Å ³	2041.16(4)	GOF on F ²	0.995
Z	4	ρ _{max} /ρ _{min} , e Å ⁻³	0.975/ -0.339
D _c , g/cm ³	2.124		

Table S2. Selected Bond Lengths (Å) and Bond Angles (°) for **1**

Bond Lengths (Å)		Bond Lengths (Å)	
Dy(1)-O(1W)#1	2.392(3)	Dy(1)-N(1)#1	2.558(3)
Dy(1)-O(1W)	2.392(3)	Dy(1)-N(3)#1	2.558(3)
Dy(1)-O(1)#1	2.456(3)	Dy(1)-N(3)	2.557(3)
Dy(1)-O(1)	2.456(3)	Dy(1)-O(2)#1	2.699(3)
Dy(1)-N(1)	2.558(3)	Dy(1)-O(2)	2.699(3)
N(6)-O(5)	1.230(5)	C(5)-C(6)	1.355(5)
Bond Angles (°)		Bond Angles (°)	
O(1W)#1-Dy(1)-O(1W)	146.52(13)	O(1W)#1-Dy(1)-O(1)#1	114.69(9)
O(1W)-Dy(1)-O(1)#1	76.12(9)	O(1W)-Dy(1)-N(1)#1	137.78(9)
O(1W)#1-Dy(1)-N(3)#1	81.12(10)	O(1)#1-Dy(1)-N(3)	139.98(9)

Symmetry Codes for **1**, #1:-x, y, 0.5-z.

Table S3. Summary of SHAPE analysis for **1**.

label	shape	symmetry	Distortion(τ)
DP-10	Decagon	D _{10h}	29.422
EPY-10	Enneagonal pyramid	C _{9v}	20.278
OBPY-10	Octagonal bipyramid	D _{8h}	22.029
PPR-10	Pentagonal prism	D _{5h}	15.868
PAPR-10	Pentagonal antiprism	D _{5d}	16.180
JBCCU-10	Bicapped cube J15	D _{4h}	10.206
JBCSAPR-10	Bicapped square antiprism J17	D _{4d}	7.351
JMBIC-10	Metabidiminished icosahedron J62	C _{2v}	11.827
JATDI-10	Augmented tridiminished icosahedron J64	C _{3v}	17.005
JSPC-10	Sphenocorona J87	C _{2v}	4.359
SDD-10	Staggered Dodecahedron (2:6:2)	D ₂	7.726
TD-10	Tetradecahedron (2:6:2)	C _{2v}	7.919
HD-10	Hexadecahedron (2:6:2) or (1:4:4:1)	D _{4h}	13.262

Table S4. H-bonding length and angle table for **1**.

D-H...A	d(H...A)(Å)	d(D...A)(Å)	<DHA(Å)
O1W-H1WA...O4	1.93(2)	2.727(4)	160(3)
O1W-H1WA...O5	2.557(18)	3.276(3)	145(3)
N2-H2...O4	2.36	3.136(4)	150
N2-H2...O4	2.50	3.219(4)	142
O1W-H1WB...O2	2.10(2)	2.889(4)	157(3)
N4-H4...O5	2.07	2.880(4)	156
O1W-H1WB...O2	2.39(2)	2.776(9)	108

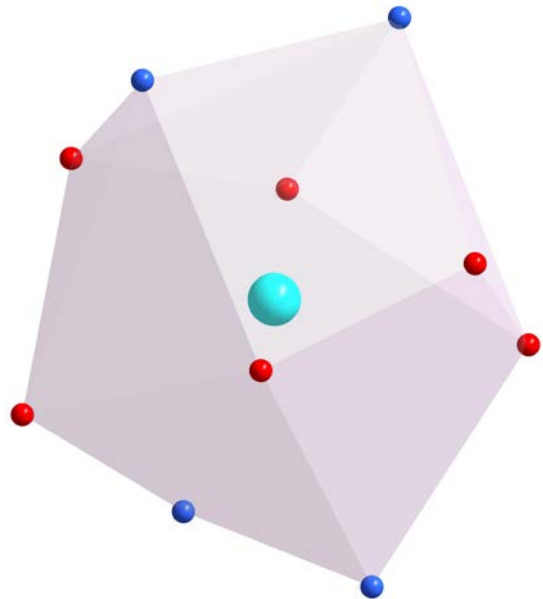


Figure S1. Sphenocorona coordination polyhedron around the Dy^{III} ion in **1**.

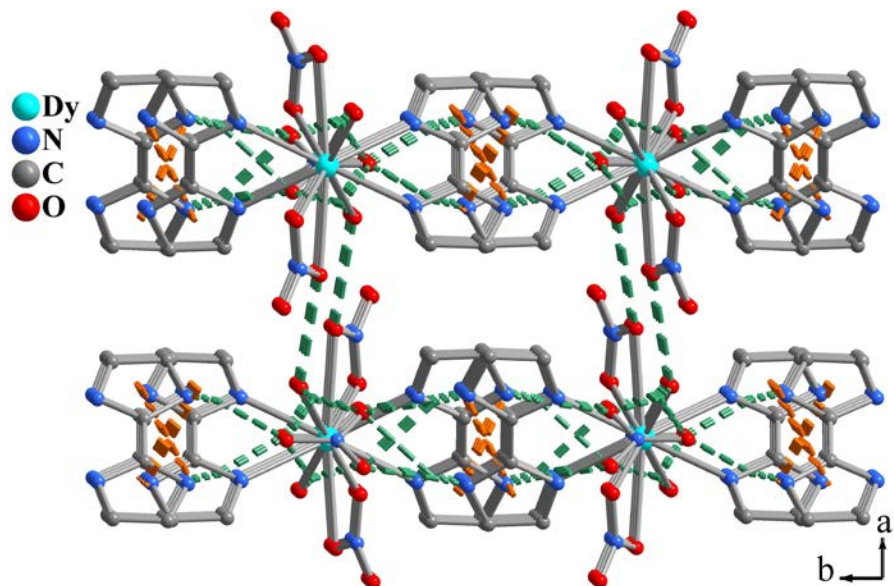


Figure S2. 3-D supramolecular network of **1** formed by H-bond along the *c*-axis (green dashed lines).

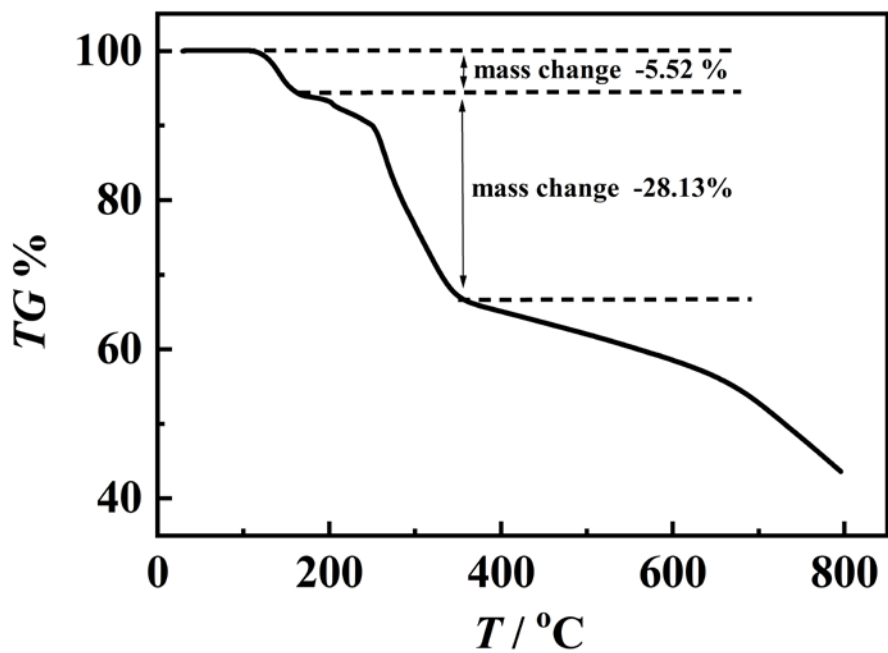


Figure S3. TGA plot of **1**.

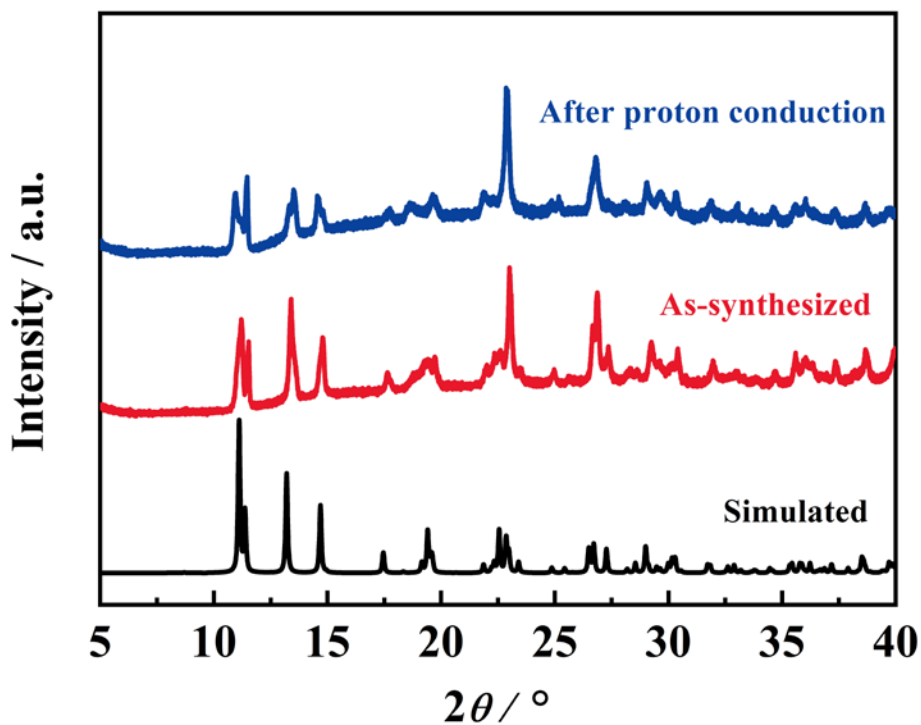


Figure S4. Powder X-ray diffraction patterns of simulated one, as-synthesized sample, the sample after proton conduction of **1**.

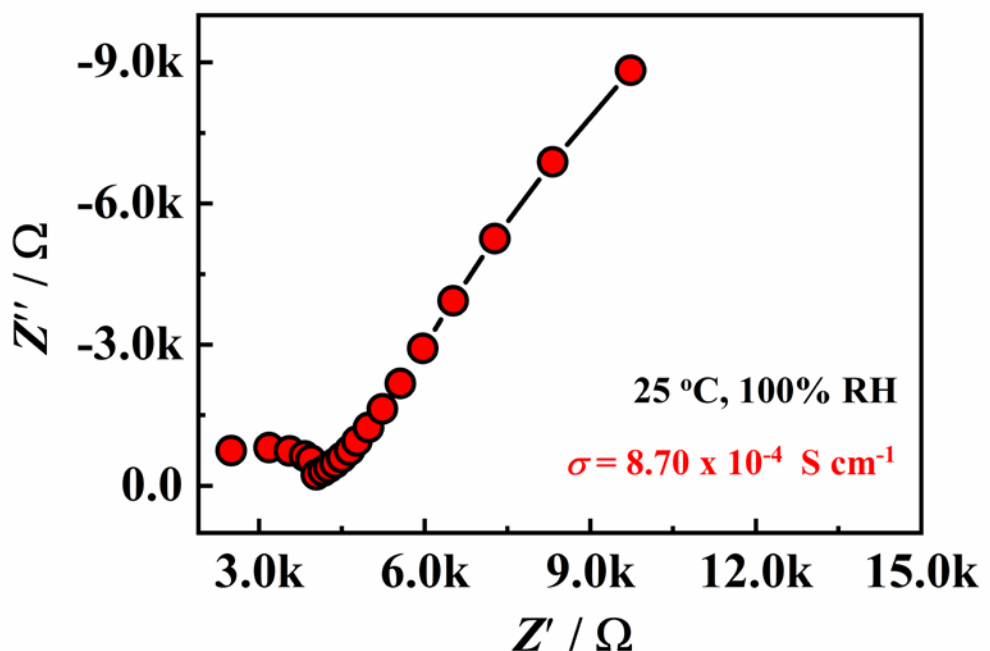


Figure S5. Nyquist plot for **1** at $25\text{ }^{\circ}\text{C}$ under 100% RH.

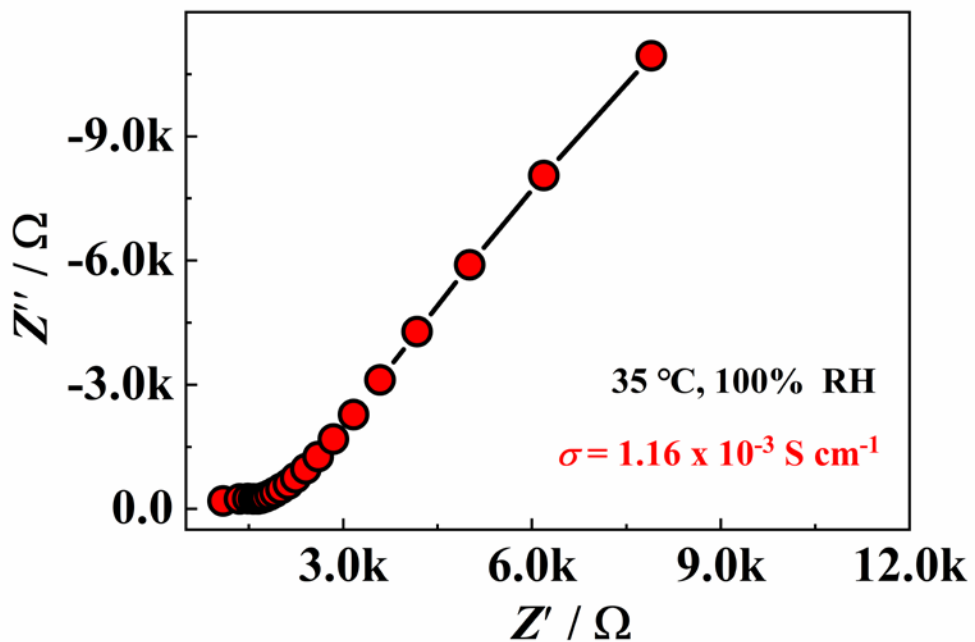


Figure S6. Nyquist plot for **1** at $35\text{ }^{\circ}\text{C}$ under 100% RH.

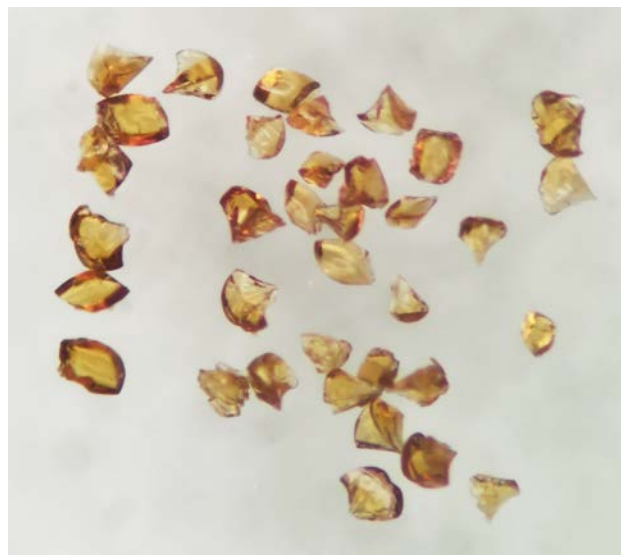


Figure S7. The photograph of crystals of complex **1** after exposed to 25-35 °C and 60-100% RH conditions during the whole proton conductivity measurements.

Table S5. Proton conductivity of **1** at 25 °C under variable relative humidity (RH).

RH / %	$\sigma / \text{S cm}^{-1}$
20	5.12×10^{-10}
30	2.47×10^{-9}
40	2.49×10^{-8}
50	1.23×10^{-7}
60	1.16×10^{-6}
70	5.73×10^{-6}
80	4.36×10^{-5}
90	2.80×10^{-4}
100	8.70×10^{-4}

Table S6. Comparison of the proton conductivity of **1** with that of imidazole/imidazole derivates-based conducting materials by using compacted pellets at relatively low temperature. σ represents proton conductivity and RH stands for relative humidity.

	Compounds	Conductivity (S cm^{-1})	Conditions (°C, RH)	References

1	[Dy(H ₂ bim) ₂ (NO ₃) ₂ (H ₂ O) ₂]·(NO ₃)	8.70×10 ⁻⁴ 1.16×10 ⁻³	25°C, 100% 35°C, 100%	This work
2	[Cr ₄ In ₄ (Himdc) ₁₂]·H ₂ O [Cr _{7.28} In _{0.72} (Himdc) ₁₂]·H ₂ O (L= 4,5-imidazole-dicarboxylate)	2.3×10 ⁻³ 2.1×10 ⁻³	22.5 °C, 98% 22.5 °C, 98%	<i>Angew. Chem. Int. Edit., 2015, 54, 7886–7890</i>
3	{Na[Cd(MIDC)]} _n (H ₃ MIDC=2-methyl-1H-imidazole-4,5-dicarboxylic acid)	1.04×10 ⁻³	100°C, 98%	<i>ACS Appl. Mater. Interfaces, 2019, 11, 1713–1722</i>
4	{[Co ₃ (p-CPhHIDC) ₂ (4,4'-bipy)(H ₂ O)] ₂ H ₂ O}{(n)} {[Co ₃ (p-CPhHIDC) ₂ (bpe)(H ₂ O)] ₃ H ₂ O}{(n)} (p-CPhH ₄ IDC=2-(4-carboxylphenyl)-1H-imidazole-4,5-dicarboxylic acid; 4,4'-bipy=4,4'-bipyridine, bpe=trans-1,2-bis(4-pyridyl)ethylene)	1.04×10 ⁻³ 7.02×10 ⁻⁴	100°C, 98% 100°C, 98%	<i>Chem. Eur. J., 2019, 25, 14108–14116</i>
5	[M ₂ (o-CPhH ₂ IDC) ₂ (H ₂ O) ₍₆₎]·4H ₂ O (M = Co (1) and Zn (2)) (o-CPhH ₄ IDC = 2-(2-carboxylphenyl)-1H-imidazole-4,5-dicarboxylic acid) and [Mn(o-CPhH ₂ IDC)(2,2'-bipy)(H ₂ O) ₂] (2,2'-bipy = 2,2'-bipyridine)	1.78×10 ⁻⁴ 1.68×10 ⁻⁴ 5.4×10 ⁻⁵	100°C, 98% 100°C, 98% 100°C, 98%	<i>Appl. Surf. Sci., 2020, 504, 144484</i>
6	[M(FPhH ₂ IDC) ₂ (H ₂ O) ₂]·4H ₂ O (M = Cd (1); Co (2)) Ni(FPhH ₂ IDC) ₂ (2,2'-bipy)]·H ₂ O (FPhH ₃ IDC = 2-(fluoro)phenyl-4,5-imidazole dicarboxylic acid, 2,2'-bipy = 2,2'-bipyridine)	2.77×10 ⁻⁴ 3.42×10 ⁻⁵ 4.61×10 ⁻⁵	100°C, 98% 100°C, 98% 100°C, 98%	<i>J. Solid State Chem., 2019, 282, 121129</i>
7	M(m ₃ -HPhIDC)(m-C ₂ O ₄) _{0.5} (H ₂ O)·2H ₂ O (M = Tb; Eu) (H ₃ PhIDC=2-phenyl-1H-imidazole-4,5-dicarboxylic acid)	8.95×10 ⁻⁴ 4.63×10 ⁻⁴	100°C, 98% 100°C, 98%	<i>Chem. Asian. J., 2019, 15, 182–190</i>
8	{[Cd(p-TIPhH ₂ IDC) ₂]·H ₂ O} _n [p-TIPhH ₃ IDC = 2-p-(1H-1,2,4-triazoly)phenyl-1H-4,5-imidazoledicarboxylic acid] [Sr(DMPPhH ₂ IDC) ₂](n) [DMPPhH ₃ IDC = 2-(3,4-dimethylphenyl)-1H-imidazole-4,5-dicarboxylic acid]	1.24×10 ⁻⁴ 9.2×10 ⁻⁴	100°C, 98%	<i>Inorg. Chem., 2019, 58, 5173–5182</i>
9	{[Mn(o-CPhH ₂ IDC)(4,4-bipy)(0.5)(H ₂ O) ₂]·3H ₂ O}{(n)} (1)	5.74×10 ⁻⁵ 5.00×10 ⁻⁵	100°C, 98% 100°C, 98%	<i>New J. Chem., 2019, 43,</i>

	$\{[Zn_5(o\text{-}CPhH_2IDC)_2(o\text{-}CPhHIDC)_2(2,2\text{-bipy})_5]\cdot 5H_2O\}_n$ (2) (o-CPhH ₄ IDC = 2-phenyl(2-carboxyl)-1-H-imidazole-4,5-dicarboxylic acid; 4,4-bipy = 4,4-bipyridine, 2,2-bipy = 2,2-bipyridine)			4859–4866
10	$[Cd(HDMPhIDC)(H_2O)]_n$ (H ₃ DMPHIDC = 2-phenyl(3,4-dimethyl)-1-H-imidazole-4,5-dicarboxylic acid)	1.30×10^{-4}	100°C, 98%	<i>New J. Chem.</i> , 2019 , 42, 20197–20204
11	$\{[CoL_2(H_2O)_2](ClO_4)_2\cdot 3DMA\cdot 0.4H_2O\}_n$ (L=bis(4-imidazol-1-ylphenyl)diazene)	3.96×10^{-4}	80°C, 95%	<i>Cryst. Growth Des.</i> , 2018 , 18, 6211–6220
12	$[Ni(Imdz)_6]_{0.5}(1,5\text{-NDS})_{0.5}\cdot H_2O$ $[Ni(Imdz)_6]_{0.5}(2,6\text{-NDS})_{0.5}$ $[Ni(Imdz)_6]_{0.5}(4,4'\text{-BPDC})_{0.5}\cdot H_2O$ (Imdz = imidazole, 1,5-NDS = 1,5-naphthalenedisulfonic acid, 2,6-NDS = 2,6-naphthalene disulfonate, 4,4'-BPDC = 4,4'-biphenyl dicarboxylic acid)	7.5×10^{-4} 3.5×10^{-4} 9.7×10^{-4}	80°C, 98% 80°C, 98% 80°C, 98%	<i>Chem. Eur. J.</i> , 2019 , 25, 1691–1695
13	$\{[Sr(o\text{-}CPhH_2IDC)(H_2O)_2]\cdot 2H_2O\}_n$	6.08×10^{-5}	100°C, 98%	<i>Polyhedron</i> , 2019 , 169, 1–7
14	$[Cu_4(HDMPhIDC)_4(H_2O)_4]_n$ (H ₃ DMPHIDC = 2-(3,4-dimethyl)phenyl-4,5-imidazole dicarboxylic acid)	2.58×10^{-5}	100°C, 98%	<i>Polyhedron</i> , 2019 , 158, 377–385
15	$[Sr(H_2PhIDC)_2(H_2O)_4]\cdot 2H_2O$ (H ₃ PhIDC = 2-phenyl-4,5-imidazole dicarboxylic acid)	1.91×10^{-6}	90°C, 98%	<i>J. Alloys Compd.</i> , 2018 , 750, 895–901
16	$[Zn(2\text{-MeBIM})_2(OAc)_2]\cdot 3H_2O$ $[Zn(2\text{-MeBIM})(Pht)(H_2O)]\cdot 2H_2O$ (2-MeBIM = 2-methyl benzimidazole, OAc = acetate anion and Pht = dianion of phthalate)	4.5×10^{-6} 1.0×10^{-5}	25°C, 100% 25°C, 100%	<i>Inorg. Chim. Acta.</i> , 2015 , 437, 167–176
17	$[Sr(H_2PhIDC)_2(H_2O)_4]\cdot 2H_2O$ (H ₃ PhIDC = 2-phenyl-4,5-imidazole dicarboxylic acid)	1.91×10^{-6}	90°C, 98%	<i>J. Alloys Compd.</i> , 2018 , 750, 895–901
18	$Zn_3(IBT)_2(H_2O)_2$ (IBT = 4,5-bis(tetrazol-5-yl)imidazole)	1.98×10^{-5}	30°C, 97%	<i>CrystEenComm.</i> , 2018 , 20, 3158–3161
19	$\{[Mn(o\text{-}CPhH_2IDC)(4,4\text{-bipy})_{0.5}(H_2O)_2]\cdot 3H_2O\}_n$ $\{[Zn_5(o\text{-}CPhH_2IDC)_2(o\text{-}CPhHIDC)_2(2,2\text{-bipy})_5]\cdot 5H_2O\}_n$ (o-CPhH ₄ IDC = 2-phenyl	5.74×10^{-5} 5.00×10^{-5}	100°C, 98% 100°C, 98%	<i>New J. Chem.</i> , 2019 , 43, 4859–4866

	(2-carboxyl)-1- <i>H</i> -imidazole-4,5-dicarboxylic acid, 4,4-bipy = 4,4-bipyridine, 2,2-bipy = 2,2-bipyridine)			
--	--	--	--	--

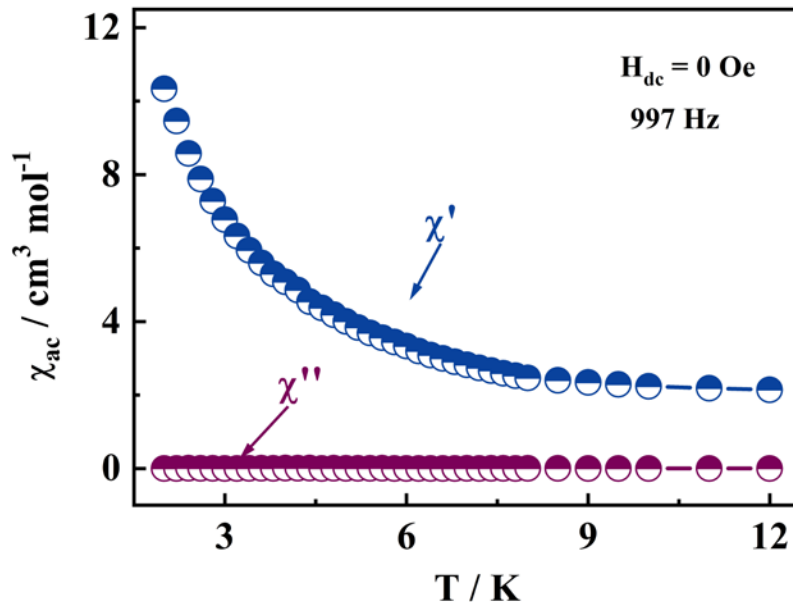


Figure S8. AC susceptibility measurements at frequency with 977 Hz for **1** at $H_{dc} = 0 \text{ Oe}$, $H_{ac} = 2.5 \text{ Oe}$

Table S7. Linear combination of two modified debye model fitting parameters from 2 to 7 K at $H_{dc} = 2000 \text{ Oe}$

T / K	$\chi_2 / \text{cm}^3 \text{ mol}^{-1}$	$\chi^1 / \text{cm}^3 \text{ mol}^{-1}$	$\chi^0 / \text{cm}^3 \text{ mol}^{-1}$	τ_1 / s	α_1	τ_2 / s	α_2
2.0	8.17013(3)	30.88637(3)	0.05932(2)	0.15681(3)	0.61197(3)	0.07813(4)	0.53235(3)
2.5	6.26158(2)	30.05776(3)	0.12518(3)	0.07798(3)	0.57477(2)	0.05504(11)	0.50642(5)
3.0	4.45468(10)	9.362200(4)	0.18504(3)	0.03917(4)	0.59412(8)	0.03087(9)	0.38119(6)
3.5	3.41827(4)	12.06544(2)	0.26272(2)	0.01892(5)	0.52011(6)	0.02244(3)	0.41470(3)

4.0	2.81495(4)	10.13028(4)	0.33112(4)	0.01100(5)	0.48396(5)	0.01581(5)	0.39021(3)
4.5	2.41554(3)	19.61455(5)	0.37435(7)	0.00800(3)	0.44415(6)	0.00963(2)	0.41420(4)
5.0	2.14388(2)	25.28558(3)	0.42505(6)	0.00517(2)	0.41641(6)	0.00590(2)	0.40128(2)
5.5	1.93974(6)	29.67630(8)	0.44859(9)	0.00310(5)	0.39878(4)	0.00342(3)	0.39020(4)
6.0	1.77070(7)	33.17694(2)	0.47873(3)	0.00139(3)	0.36814(3)	0.00149(5)	0.36404(2)
6.5	1.63772(8)	46.78638(7)	0.49054(4)	0.00051(5)	0.34091(3)	0.00053(3)	0.33988(3)
7.0	1.53205(3)	102.80047(6)	0.51386(4)	0.00020(8)	0.31607(2)	0.00020(7)	0.31584(6)

Table S8. The comparisons of the proton conductivity and the U_{eff}/k values of **1** with the previously reported proton-conductive nanomagnet. RH represents for relative humidity.

	Compounds	Proton Conductivity	U_{eff}/k	References
1	$[\text{Dy}(\text{H}_2\text{bim})_2(\text{NO}_3)_2(\text{H}_2\text{O})_2] \cdot (\text{NO}_3)_3$	$8.70 \times 10^{-4} \text{ S} \cdot \text{cm}^{-1}$ under 25°C and 100% RH $1.16 \times 10^{-3} \text{ S} \cdot \text{cm}^{-1}$ under 35°C and 100% RH	71.6 K for the FR phase and 74.4 K for the SR phase at $H_{\text{dc}} = 2000 \text{ Oe}$.	This work
2	$[\text{Dy}_{72}(\text{mda})_{24}(\text{mdaH})_8(\text{OH})_{120}(\text{O})_8(\text{NO}_3)_{16}] \cdot (\text{NO}_3)_8 \cdot 16\text{CH}_3\text{OH} \cdot 168\text{H}_2\text{O}$ (mdaH ₂ = N-methyldiethanolamine)	$1.80 \times 10^{-3} \text{ S} \cdot \text{cm}^{-1}$ under 25°C and 95% RH	19.6 K at $H_{\text{dc}} = 0 \text{ Oe}$	<i>Adv. Mater.</i> , 2016 , 28, 10772–10779
3	$(\text{H}_5\text{O}_2)_2(\text{H})[\text{Yb}^{\text{III}}(\text{hmpa})_4][\text{Co}^{\text{III}}(\text{CN})_6]_2 \cdot 0.2\text{H}_2\text{O}$ (HDBM = 1,3-diphenyl-propane-1,3-dione)	$1.74 \times 10^{-4} \text{ S} \cdot \text{cm}^{-1}$ under 25°C and 97% RH	31.2 K at $H_{\text{dc}} = 1000 \text{ Oe}$	<i>J. Am. Chem. Soc.</i> , 2020 , 142, 3970–3979

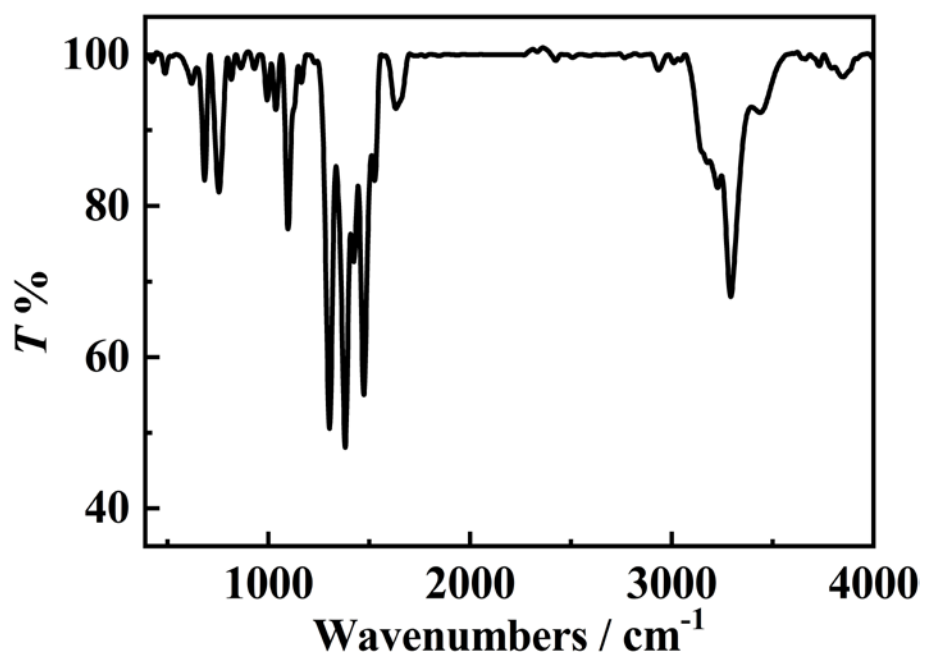


Figure S9. IR spectra for **1**.